5-2013

Stochastic Simulations of the Mitogen-Activated Protein Kinase Cascade: On Chemical Waves as a Mechanism for Signal Transduction

Daniel Case

Stochastic Simulations of the Mitogen-Activated Protein Kinase Cascade: On Chemical Waves as a Mechanism for Signal Transduction

by

Daniel Case

Undergraduate honors thesis under the direction of

Dr. Dana Browne

Submitted to the LSU Honors College in partial fulfillment of the Upper Division Honors Program.

May, 2013

Louisiana State University
& Agricultural and Mechanical College
Baton Rouge, Louisiana

Contents

Abstract

The biochemical reactions that make up the three-tiered mitogen-activated protein kinase (MAPK) cascade are known to occur in different spatial regions within the cell. As a result, it has previously been found, through deterministic simulations, that signal transduction through this pathway may occur via chemical waves that emerge because of bistability in the cascade. Here, stochastic simulations confirm the emergence of these waves when bistability is present. Further, the properties of bistability that promote wave propagation are examined in detail. I found that the primary determinant of successful signal transduction through wave propagation is the steady state spatial profile of the activator (ppMAP2K) of the protein that makes up the chemical wave (ppMAPK). The advantage provided by bistability in the final tier of the cascade is that steady states with high [ppMAPK] in regions of low [ppMAP2K] exist. This property of bistability allows the wave to propagate through regions of the cell where [ppMAP2K] is characteristically low. In addition, feedback mechanisms added to the model that improve wave propagation do so by significantly altering the spatial profile of [ppMAP2K] inside the cell. Finally it is shown that chemical waves are able to propagate even when bistability is not present, as long as [ppMAP2K] is sufficiently high throughout the cell.

1 Introduction

How living cells process large amounts of information about their environment in short periods of time remains to be well understood. It is known that cells are able to do so since cellular responses to environmental changes are observable in the laboratory. Information is presented to the cell in the form of small molecules colliding with the cell membrane, the cell's semi-permeable barrier to the outside world. These small molecules that provide a signal could be hormones, insulin, epinephrine, or some other stimulus that incites a cellular response. However, in order for the cell to issue a response, the signal must reach the cell's nucleus, where specific actions take place depending on what information is received. Therefore, the information must be transferred from the membrane to the nucleus through a signal transduction pathway, a series of biochemical reactions that carries the information about what outside stimulus was received. These pathways are often highly complex, and not well mapped; however, they are prime examples of systems that transmit information through space, but are not electronic, electronic systems being what we are most used to. Rather, these systems are grounded in chemistry. Here, I examine the mechanism employed by the transduction pathway that allows the signal to be carried through space.

One of the primary types of signal transduction pathways is the phosphorylation cascade. In a linear cascade of this type, each protein in a specific set is able to take on one of two forms at any time, an active form and an inactive form. A protein in this set can transition from inactive to active form by the addition of a phosphorous group at some location on the protein: a mechanism called phosphorylation. This is most commonly executed through a process where the inactive protein and an ATP molecule (the source of the phosphorous group) bind to the activated form of another type of protein. The activated protein facilitates the transfer of the phosphorous group from the ATP molecule to the inactive protein. The active protein then releases the now ADP molecule and the newly activated protein. The initially active protein as well as the newly activated protein are then able to go and catalyze the activation of other proteins. Similarly, dephosphorylation is the removal of a phosphorous group from a protein, which transitions the protein from its active form to its inactive form. This process occurs when an active protein binds to another type of protein called a phosphatase. The phosphatase facilitates the removal of a phosphorous group from the active protein and then releases the inactive protein. The phosphatase is then free to dephosphorylate another active protein, and the newly deactivated protein is free to be reactivated.

Typically in a phosphorylation cascade, an extracellular molecule collides with the cell membrane and binds to a specific type of receptor protein on the membrane. This receptor is partly inside of the cell and will phosphorylate the first protein type in the cascade. These newly activated proteins will then activate the next type of protein in the cascade, which will then activate the next type, and so on. The cascade is linear in the sense that there is a certain sequence in the types of proteins that become activated, it is a consecutive process; each type of active protein is only able to activate one other type of protein. In this study, the signal is considered to be transduced once the concentration of the active form of the final protein in the cascade reaches a threshold level near the nucleus.

Simple, linear, phosphorylation cascades were given a mathematical structure by Heinrich et. al [1]. The cascade is initiated by a receptor that has decaying activity in time. The temporal change in the concentration of the active form of any protein in the cascade is dependent only on a rate constant, the concentration of the inactive form of the protein, and the concentration of the active form of the preceding protein in the cascade. The deactivation of a protein depends only on a rate constant and the concentration of the active form of that protein. Through analysis, this model showed the possibility of signal amplification or attenuation simply through adjustments in the values of the rate constants.

The underlying assumption of this model is that the cytosol containing each of the proteins in the cascade is well mixed. Further, only temporal dynamics are explored, spatial organization is unaccounted for. For example, the receptor is not restricted to being membrane-bound in this model. The linearity of the model also does not allow for any feedback mechanism within the cascade.

Huang and Ferrell proposed a model for the mitogen-activated protein kinase (MAPK) cascade that was supported by their experimental work on *Xenopus* oocytes [2]. This cascade consists of three proteins: MAP3K, MAP2K, and MAPK, the latter two of which require double phosphorylation in order to convert the protein to its active form. It is this distinction that provides novel dynamics in

active protein concentration levels when compared to the Heinrich model. The double phosphorylation acts as an effective feedback characteristic. Each phosphorylation requires a separate collision with the activating protein, and the phosphatase only removes one phosphorous group at a time. Further, the model considers the time the molecules remain in complexes by assigning rate constants to both the formation of a complex and to the dissociation of the complex into products. What was found is that while MAP3K follows a Michaelis-Menten pattern as the concentration of the activator of MAP3K is increased, MAP2K and MAPK display consecutively steeper sigmoidal patterns. The activator of MAP3K is analogous to the receptor in the Heinrich model. MAPK was found to be ultrasensitive or switch-like in this model.

What fails to be considered here also is the spatial dynamics of the cascade. The cytosol is still considered to be well mixed, so the effect of spatial localization of any element of the cascade was not investigated. The spatial separation of activation and deactivation mechanisms has been known to be an important characteristic of transduction pathways, and Kholodenko examined this characteristic for simple, linear phosphorylation cascades, like those discussed by Heinrich [3],[4]. Essentially, the initial activator of the cascade is a membrane-bound receptor. This receptor activates the first protein; this protein can then diffuse into the cytosol where it can activate the next protein in the cascade but will eventually be dephosphorylated. It was found that diffusion alone severely limits the transduction of the signal through the cytosol. The concentration of the active form of each protein drops off exponentially with from the membrane. Therefore diffusion cannot sole mechanism of signal transduction in such a cascade. The cell must utilize other mechanisms such as endocytosis, motor proteins, or scaffolding proteins in order for the signal to be spatially transduced.

At the time, Kholodenko did not investigate the dynamics of a feedback mechanism such as the double phosphorylation step in the MAPK cascade. Later, Kholodenko et al, using the MAPK model proposed by Huang and Ferrell, found numerically that a single module of the MAPK cascade that includes double phosphorylation can display bistability under certain parameter values [5],[6]. Bistability was the only bifurcation found in the study.

Kholodenko, Markevich, et al. later found that from this bistability can emerge protein waves that start from the membrane, where initial activation of the cascade takes place, and move through the cytosol [7]. This is a novel method of signal transduction for phosphorylation cascades, and is one that does not require additional mechanisms such as scaffolding or motor proteins. It should be noted however, that in other physical settings, chemical waves have been found to emerge as a result of bistability [8]. Chemical waves allow for a signal to be transmitted over long distances which was not possible by way of diffusion only. The approach taken by Kholodenko et al. in their analysis was to use reaction-diffusion equations with Michaelis-Menten kinetics. Therefore their model was inherently deterministic. Further, the reason bistability produced propagating waves was not explained. They did find conditions under which bistability alone failed to produce a propagating wave front and proposed two positive feedback mechanisms which work in tandem with bistability to produce a wave under such conditions.

Here, I use a stochastic model to simulate the MAPK cascade using elementary rate steps instead of Michaelis-Menten kinetics. The purpose is to determine whether bistability is capable of producing propagating waves in a noisy setting. Further, I look closer at the mechanism which explains why bistability produces a wave front and how changes in geometry and initial concentrations that do not disturb the bistability characteristic affect wave propagation. Finally, I examine the two alternative mechanisms of positive feedback proposed by Markevich, et al. in an effort to explain how they complement bistability in the cascade and produce a propagating wave under conditions where bistibility alone was insufficient in doing so.

2 Model

2.1 Background

The model of the MAPK cascade first proposed by Huang and Ferrel is shown in Figure 1. Each reaction in the cascade occurs in a specific region of the cell, as summarized in Table 1.

To simplify the discussion of the details of this cascade I am temorarily switching to a simplified

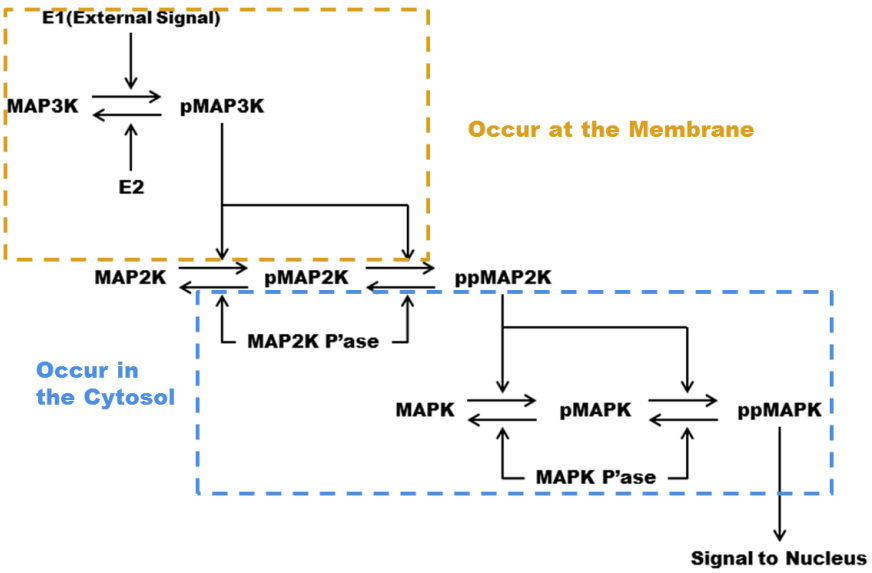

Figure 1: The MAPK Cascade. Reactions within the same dashed boxes occur in the same spatial region of the cell.

Molecule	Location	Activation Location	Deactivation Location
E1	External	-	-
E2	Membrane	-	-
MAP3K	Membrane	Membrane	Membrane
MAP2K	Cytosol	Membrane	Cytosol
MAP2K P'ase	Cytosol	-	-
MAPK	Cytosol	Cytosol	Cytosol
MAPK P'ase	Cytosol	-	-

Table 1: MAPK Cascade Details. Summary of where each type of molecule in the cascade is physically present in the cell.

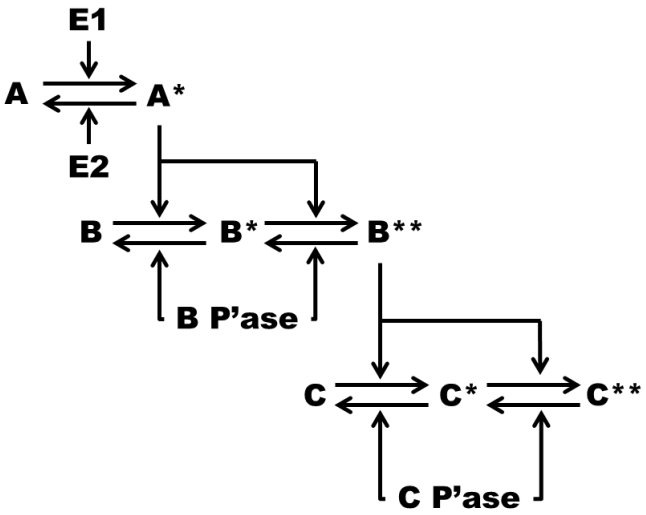

Figure 2: MAPK Cascade with Simplified Notation. This figure is analogous the Figure 1. "*" and "**" imply single and double phosphorylation respectivly, i.e. **A** ≡ MAP3K, **B*** ≡ pMAP2K, **C**** ≡ ppMAPK, etc.

notation. A diagram of the cascade with this notation is shown in Figure 2 and is completley analogous to Figure 1. The following is a walk through of the dynamics of the cascade.

1. In this pathway, a signal is triggered by an external chemical (**E1** in Figure 2) that activates the membrane bound molecule **A**, transforming **A** to **A***.

2. **A*** remains bound to the cell membrane and may be deactivated by a second chemical **E2** that is also membrane bound.

3. **B** is present in the cytosol and must react with **A*** on the membrane in order to be activated. Once activated, **B*** is free to diffuse through the cytoplasm. However, in order for **B*** to be transformed to **B**** it must once again react with **A*** on the membrane; likewise, **B**** is able to diffuse through the cytosol.

4. The deactivator of **B*** and **B****, called B Phosphatase (**B P'ase**) is distributed throughout the cytosol. Therefore as **B*** and **B**** diffuse through the cytosol they are prone to deactivation.

5. **C** is present in the cytosol and is transformed to **C*** and then to **C**** through two separate reactions with **B****.

6. Finally, **C*** and **C**** are deactivated by C Phosphatase (**C P'ase**) that is located in the cytosol.

In order for the cell to respond to an external signal, information about that signal must reach the cell nucleus. For this signaling pathway, the information is considered to be successfully relayed to the nucleus when a high concentration of **C**** (ppMAPK) reaches the nucleus, as this will stimulate a cellular response to the external signal. The concentration of **C**** is considered to be high at the nucleus when it is close to the same value as at the cell surface in the steady state. In this study I investigate the temporal and spatial properties of the chemical mechanism in this pathway that achieves a high concentration of **C**** at the nucleus.

The reason that the accomplishment of a high [**C****] at the cell nucleus is not a trivial one is that the conversion of **C** to **C**** requires reactions with **B****. Since **B**** is only created at the outer membrane and deactivated everywhere within the cytosol, the concentration of **B**** tends to rapidly decrease with distance from the membrane. Because there is a uniform concentration of **C P'ase** throughout the cytosol, areas with a high rate of **C** activation (high [**B****]) will have high concentrations of **C****, while areas with a low rate of **C** activation (low [**B****]) will have low concentrations of **C****. Examples of two such areas are the cytosol near the outer membrane and the cytosol near the nucleus, respectively.

Previously Markevich et al. found, using deterministic reaction-diffusion equations and Michaelis-Menten kinetics, that signal transduction occurred only when bistability existed in the third tier of the cascade [7]. Further, the mechanism found in the analysis was a chemical wave front of **C**** that propagated inward from the cell membrane toward the nucleus. Here, I investigate whether stochastic simulations using elementary rate steps provide similar results, and determine the reason why bistability, at first, appears to be a prerequisite for signal transduction in the MAPK cascade.

2.2 Approach to Model Investigation

Simulations of the MAPK cascade were performed in three dimensions using different geometries. Each chemical species was represented with a discrete point particle that was able to diffuse freely through space. Elementary rate constants are used for all reactions occurring within the cytoplasm. Therefore, the occurrence of a bimolecular reaction results in the formation of a complex that, on its own, is able to diffuse freely. The complex will at some point undergo either a forward reaction, in which the complex will break into two chemical species with one species transformed from its initial form, or the complex will undergo the reverse reaction, separating into the initial two species with no transformation occurring.

Since the focus of this study is on determining the mechanism and conditions necessary for a high concentration of **C**** to be present at the outer membrane and spread to the nucleus, certain simplifications to the model were made. I considered there to be a static concentration of **A*** located on the cell surface. This eliminated the proteins **E1**, **E2**, and **A** from Figure 2. Further, the activation of **B** and **B*** at the membrane did not result in the formation of an intermediate complex. Rather, **B** was transformed to **B*** (and **B*** to **B****) if it came within the binding radius of an **A*** molecule on the membrane. Finally, each simulation was run as if the external stimulus had just been received at the

beginning of the simulation. There was no transient nature to the external signal, it was considered to be present and constant throughout the duration of the simulation.

I will now drop the simplified notation and return to the molecule names shown in Figure 1. However, most of the following discussion revolves around ppMAP2K, MAP2K P'ase, and ppMAPK, which have so far been signified as **B****, **B P'ase**, and **C****, respectively.

2.3 Michaelis-Menten vs. Elementary Rate Steps

Most past research on signal transduction pathways was performed through the use of partial differential equations. In these equations the chemical kinetics are described by Michaelis-Menten kinetics. However, in a stochastic simulation with single molecule detail, elementary rate steps must be used and it is worth understanding the difference between these two approaches, and the assumptions that must be made when Michaelis-Menten kinetics are employed.

Consider the following chemical reaction

$$\mathrm{E+S} \underset{d}{\overset{a}{\rightleftharpoons}} \mathrm{E*S} \xrightarrow{k} \mathrm{E+P}$$

where an enzyme E and substrate S combine to form the complex E∗S, then break down to E and the product P.

The concentration of free or unbound E can be represented by $[\mathrm{E}]_{Total}$-[E∗S], where $[\mathrm{E}]_{Total}$ is the total enzyme concentration (free and substrate-bound). Therefore, by the law of mass action, the rate of [E∗S] formation is equal to $a([\mathrm{E}]_{Total}\text{-}[\mathrm{E*S}])[\mathrm{S}]$. Similarly, the rate of [E∗S] breakdown is equal to $d[\mathrm{E*S}]+k[\mathrm{E*S}]$. Finally, the rate of product formation is equal to $k[\mathrm{E*S}]$. The underlying assumption of Michaelis-Menten kinetics (called the steady-state assumption) is that [E∗S] is constant. This means that the rate of formation and the rate of breakdown of [E∗S] are equal. Therefore,

$$a([\mathrm{E}]_{Total}\text{-}[\mathrm{E*S}])[\mathrm{S}]=d[\mathrm{E*S}]+k[\mathrm{E*S}].$$

This relationship simplifies to

$$[\mathrm{E*S}]=\frac{[E]_{Total}[S]}{\frac{d+k}{a}+[S]}.$$

Multiplying both sides by k to get an expression for the rate of product formation and using the Michaelis constant, $K_m \equiv \frac{d+k}{a}$, results in the following expression,

$$k[\mathrm{E*S}]=\frac{d}{dt}[\mathrm{P}]=\frac{k[E]_{Total}[S]}{K_m+[S]}.$$

To achieve the well known Michaelis-Menten equation, two other identities are used: $V_{max} \equiv k[\mathrm{E}]_{Total}$, and $V_0 \equiv k[\mathrm{E*S}]$. Using these identities we arrive at

$$\frac{d}{dt}[\mathrm{P}]=V_0=\frac{V_{max}[S]}{K_m+[S]}.$$

As already stated, I use elementary rate steps in the simulations since actual molecules are used instead of concentration values. Another reason to not use Michaelis-Menten kinetics is that throughout most of the simulation the system is not in a steady state. This violates the primary assumption from which the above equation was derived. Therefore, the elementary rate equation for product formation is $\frac{d}{dt}[\mathrm{P}]=k[\mathrm{E*S}]$. The rate is directly dependent on the current concentration of the complex E∗S, which changes over time. This equation for the rate of product formation of course becomes more complex when there is more than one reaction taking place. An example is provided in the Appendix.

2.4 Bistability in the Cascade

An important feature of the MAPK cascade is that with certain values for the elementary rate constants, the third tier of the cascade can exhibit bistability. The temporal dynamics of the third tier of the cascade are described by a set of nonlinear differential equations. This set of equations can be separated from the equations that describe the other tiers of the cascade, and the value of [ppMAP2K] can be fixed at any positive value. When these equations are solved for their steady state solutions, separate from

the rest of the cascade, there exist multiple solutions for [ppMAPK] when the value of [ppMAP2K] is between 15 and 32nM, as shown in Figure 3. The range of [ppMAP2K] from 15 to 32nM is the bistable region. Within this region there exists three steady state solutions for [ppMAPK]. The high and low value solutions (roughly 270nM and 10nM, respectively) are stable, while the intermediate value is an unstable equilibrium. The inset plots in Figure 3 are meant to display qualitative and analogous free energy diagrams of the system. Within the bistable region one would expect to see two stable equilibria and one unstable equilibrium, and at the extremities of the bistable region the free energy diagram is such that only one equilibrium exists, and that equilibrium is stable.

For consistency, the same total concentrations of MAPK and MAP2K as were used in the analysis by Markevich et al.[7] are used in this stochastic model. Further, elementary rate constants used here provide a bifurcation diagram similar to theirs in that the bistable regions closely agree. What had to be added to the simulations were molecules that represented the complexes formed as a result of bimolecular reactions in the cytosol and specific concentrations of the phosphatases. The reaction equations with the corresponding parameters are provided in Tables 2 and 3 located in the Appendix.

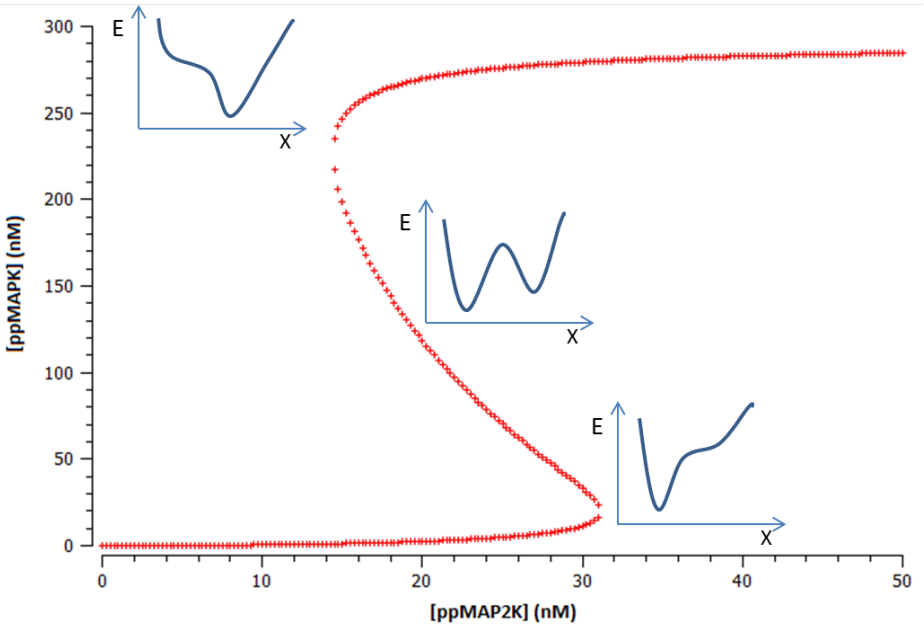

Figure 3: Bistability in the third tier of the MAPK Cascade. When [ppMAP2K] is between 15 and 32nM, the system has 3 steady state solutions for [ppMAPK]. The high and low values of [ppMAPK] (roughly 270nM and 10nM, respectivly) are stable equilibria, the intermediate values are unstable. Insets show qualitative, analogous free energy diagrams of the system, X represents [ppMAPK].

2.5 1-Dimensional Wave Propagation

The chemical wave mechanism found by Markevich et al.[7] successfully propagated the signal when in spherical geometry, however, the wave did not propagate when tested in 1-dimension. To test for wave propagation in 1-dimension with my stochastic model, I used a long three-dimensional box with square cross-section initially filled with uniformly distributed concentrations of MAPK, MAPK P'ase, MAP2K, and MAP2K P'ase, and a uniform distribution of pMAP3K was placed on the face of the box at one end (I refer to this face of the box as the activation surface). The simulation environment is shown in Figure 4.

Figure 5 shows the time evolution and steady state values of [ppMAPK] at evenly spaced distances from the activation surface for two different concentrations of MAP2K P'ase. In general, a higher concentration of MAP2K P'ase leads to faster deactivation of ppMAP2K, and hence slower creation of ppMAPK.

In the steady state, [ppMAPK] near the activation surface was over 250nM. However, in both scenarios this concentration fell below 150nM at distances further than 15-20μm from the activation

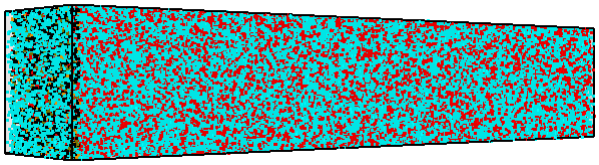

Figure 4: Simulation environment for a long box with square cross section used to simulate 1-dimension. The left square face contains evenly distributed pMAP3K (I refer to this face of the box as the activation surface), while MAP2K, MAPK, MAP2K P'ase, and MAPK P'ase are distributed uniformly throughout the box. Each colored dot represents a molecule

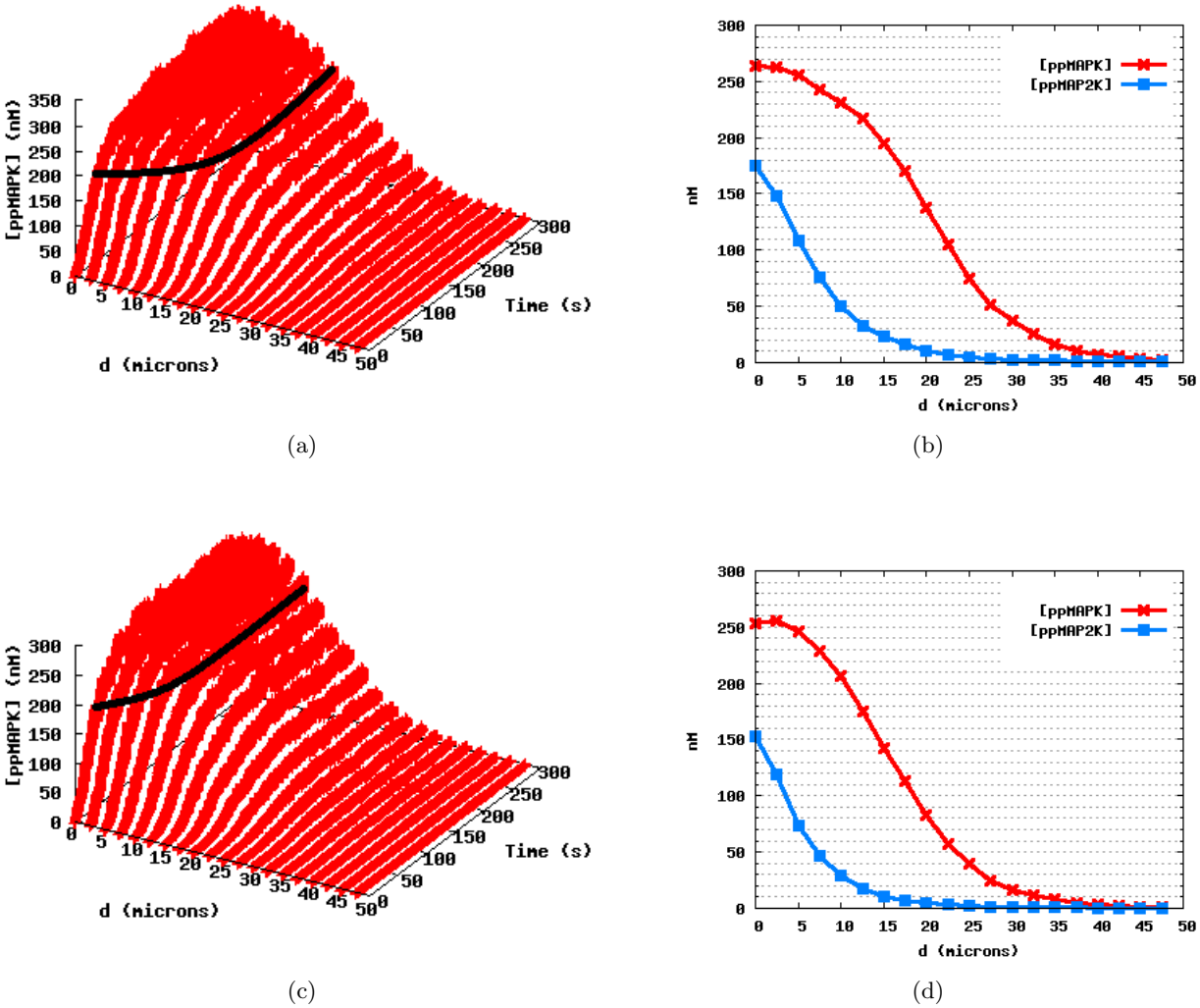

Figure 5: Time evolution of [ppMAPK] and steady state profiles of [ppMAP2K] and [ppMAPK] in 1-Dimension for two different concentrations of MAP2K P'ase: (a), (b) [MAP2K P'ase]=10nM, and (c), (d) [MAP2K P'ase]=24nM. Black contour lines at [ppMAPK]=200nM show the spatial limit of wave propagation. Higher [MAP2K P'ase] reduces the steady state spatial profile of [ppMAPK] and [ppMAP2K]

surface. Beyond 40μm from the surface, [ppMAPK] fell to near zero. In terms of distance from the surface, prior to the drop off in [ppMAPK] is a rapid decline in [ppMAP2K]. In fact, in both scenarios, beyond 20μm [ppMAP2K] fell below the bistable region ([ppMAP2K]<15nM). This means that beyond this distance the only steady state value for [ppMAPK] is near zero, as shown in Figure 3. Since [ppMAPK] eventually falls to zero, this is a wave that does not propagate indefinitely in

1-dimension.

I found that raising the concentration of MAP2K P'ase had the expected outcome of [ppMAP2K] falling to near zero levels closer to the activation surface than before. This simultaneously reduced the steady state concentration of ppMAPK at these distances. These effects can be observed by comparing Figures 5(a) and 5(d). Essentially, increasing or decreasing the uniformly distributed MAP2K phosphatase concentration produced different steady-state spatial profiles of [ppMAP2K]. These different spatial profiles of [ppMAP2K] in turn produced different steady state spatial profiles of [ppMAPK]. Overall, no scenario supported sustained wave propagation in this geometry, which agrees with previous findings.

2.6 Spherical Geometry

The condition where wave propagation was found by Markevich et al.[7] to occur as a result of bistability was in a spherical geometry, where the entire surface of the sphere served as an activation region for MAP2K. I set up the stochastic model in a similar way, in that pMAP3K was distributed uniformly over the entire surface of the sphere. The cell was represented by a sphere of radius 50μm with an excluded volume in the center taken up by a sphere of radius 20μm that served as the nucleus. The volume between the two spheres was equivalent to that of the box previously discussed in the 1-dimensional case. Figure 6 shows the simulation environment for this scenario.

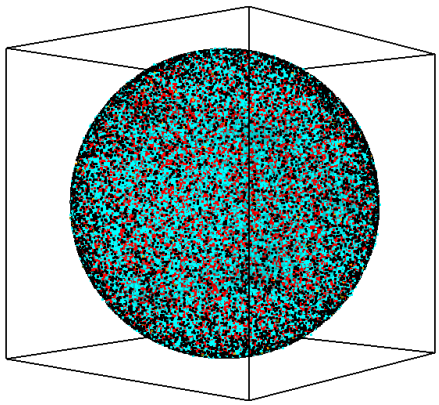

Figure 6: Simulation environment for spherical geometry. The nucleus is not visible. Black dots on the surface of the sphere represent pMAP3K molecules.

The method of varying the MAP2K phosphatase concentration was again employed in order to generate different steady state spatial profiles of [ppMAP2K], as shown in Figures 7-10. The wave propagated successfully when [MAP2K P'ase] was 10nM, as seen in Figure 7. The steady state concentration of ppMAPK is the same at the cell surface and cell nucleus. In 1-dimension under the same conditions [ppMAPK] fell below 200nM at a distance of 15μm from the activation surface, and [ppMAP2K] fell below the bistable region 17μm from the surface. However, in spherical geometry, [ppMAP2K] was in or above the bistable region throughout the entire cell. Time slices from Figure 7(a) are shown in Figure 8, illustrating the propagation of the wave through the cytosol.

Figures 9 and 10 show simulations using spherical geometry, but with higher concentrations of MAP2K P'ase. As a result, the steady states show that [ppMAP2K] fell below the bistable region much closer to the membrane and high [ppMAPK] was not sustained throughout the cell. The higher the value of [MAP2K P'ase], the closer to the surface [ppMAP2K] fell to near zero, and the shorter the wave propagation distance.

What is seen is that even though bistability is present, a high concentration of ppMAPK at the nucleus is not achieved unconditionally. Cases where the wave did not propagate to the cell nucleus also had the characteristic of having a ppMAP2K concentration below the bistable region throughout the majority of the cytosol. Figure 9(b) shows a distinct drop in [ppMAPK] after 12μm inward from the membrane, aligning with where [ppMAP2K] fell below the bistable region.

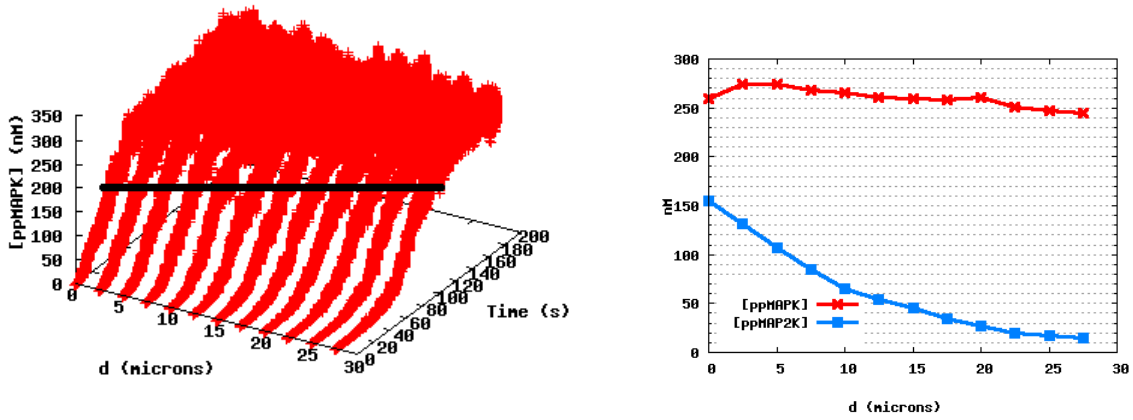

(a) (b)

Figure 7: (a) Time evolution of [ppMAPK] and (b) steady state profile of [ppMAP2K] and [ppMAPK] in spherical geometry under the condition:[MAP2K P'ase]=10nM. High [ppMAPK] throughout the cell in the steady state shows successful signal propagation. Steady wave propagation is also shown by the black contour line at [ppMAPK]=200nM in (a).

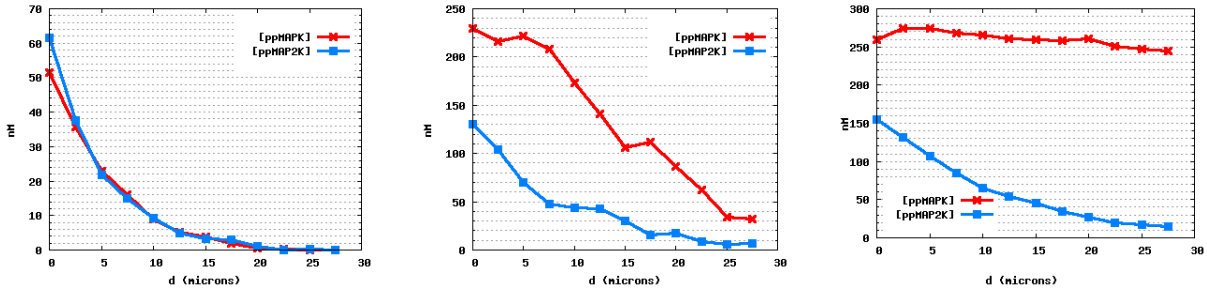

(a) (b) (c)

Figure 8: Propagation of the wave of [ppMAPK] through the cytosol in spherical geometry with [MAP2K P'ase]=10nM. Shown are the spatial profiles of [ppMAPK] and [ppMAP2K] at (a) 20 seconds, (b) 70 sec, and (c) 150 seconds.

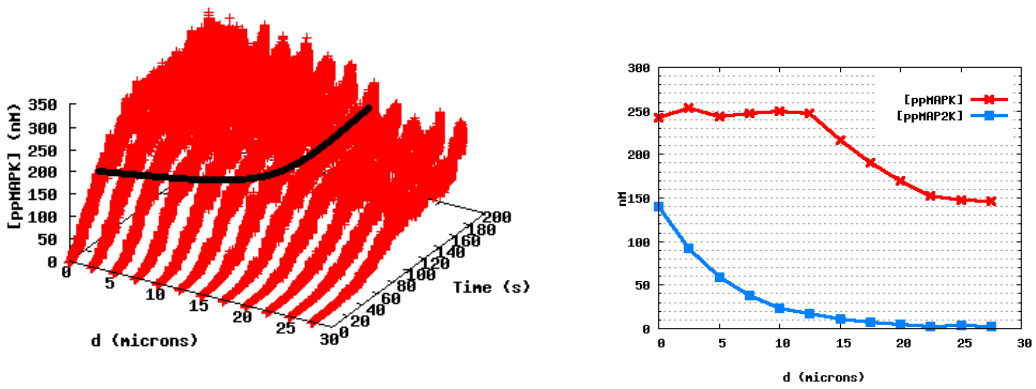

(a) (b)

Figure 9: (a) Time evolution of [ppMAPK] and (b) steady state profile of [ppMAP2K] and [ppMAPK] in spherical geometry under the condition:[MAP2K P'ase]=24nM. The contour line at [ppMAPK]=200nM in (a) shows the failure of strong signal propagation beyond 15μm from the cell surface. (b) shows a significant decline in [ppMAPK] in regions where [ppMAP2K] is below the bistable region.

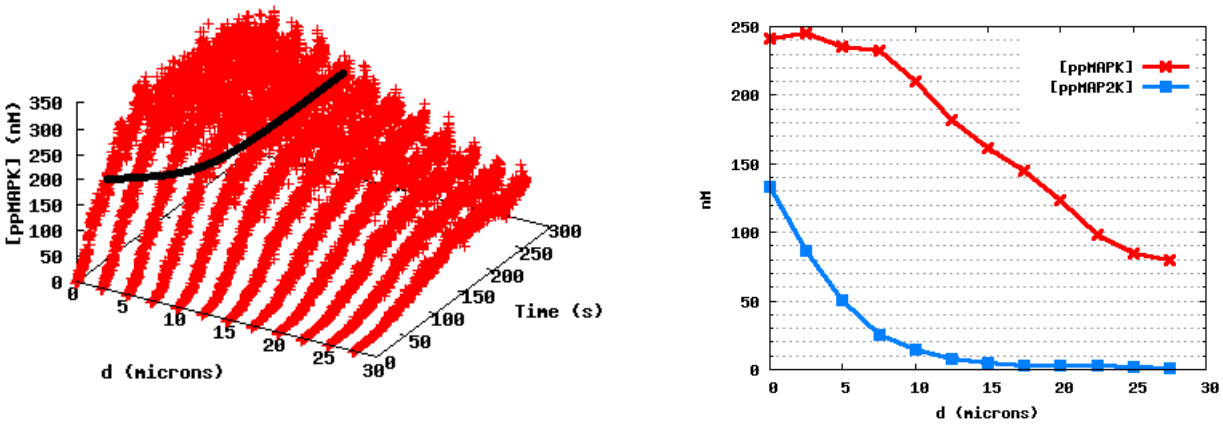

(a) (b)

Figure 10: (a) Time evolution of [ppMAPK] and (b) steady state profile of [ppMAP2K] and [ppMAPK] in spherical geometry under the condition:[MAP2K P'ase]=35nM. The contour line at [ppMAPK]=200nm in (a) shows the failure of signal propagation beyond 10μm from the cell surface. Further, (b) shows a significant decline in [ppMAPK] in regions where [ppMAP2K] is below the bistable region (beyond 10μm from cell surface).

2.7 Localized Activation

A scenario not investigated previously was localized MAP2K activation regions on the cell surface, in contrast to the entire surface being an activation region. This is a more realistic scenario because cells are often compartmentalized by internal membranes, and external signal receptors are typically not evenly distributed over the entire surface. Often times, as this scenario attempts to simulate, signal receptors are localized to regions of the cell surface. This scenario also acts as a test of the robustness of the mechanism. For in general, the condition under which the entire cell surface acts as an activation region most facilitates wave propagation, while activation restricted to a small point least facilitates wave propagation.

I performed simulations for 3 cases of localized activation. In each, I use the same concentration of pMAP3K, but define differently the area in which pMAP3K is present. In the first case, only a single region the size of 1% of the cell surface contained pMAP3K, in the second case a 7% region was used, and in the third case seven 1% regions were distributed evenly over the surface. Other than the localized activation zones, all concentrations and rate constants were unchanged and were such that a wave successfully propagated through the cytosol when pMAP3K was distributed over the entire surface (as seen in Figure 7). To illustrate, Figure 11 shows the simulation environment when the activation region is restricted to 7% of the cell surface.

The resulting steady states for these three cases of localized activation are shown in Figures 12 and 13. I found that if activation of MAP2K is restricted to a region of 1% of the cell surface the wave is attenuated prior to reaching the nucleus; however, a single 7% region was sufficient for initiating wave propagation. Finally, I found that distributed activation regions produced a weaker signal than when combined.

Impressively, these findings indicates that even with a drastic reduction in the region of the surface containing pMAP3K (7%, down from 100%), wave propagation from the membrane to the nucleus is still possible. The previous observation that successful propagation occurs when [ppMAP2K] is in or above the bistable region is consistent with this scenario, as shown in Figure 12(b). Likewise, in the case where propagation failed, Figure 12(a), [ppMAP2K] fell below the bistable region halfway between the surface and nucleus. The distributed activation zones produced a spatial profile such that [ppMAP2K] was in or above the bistable region for 60% of the distance between the surface and the nucleus. The resulting signal was diminished but still significant.

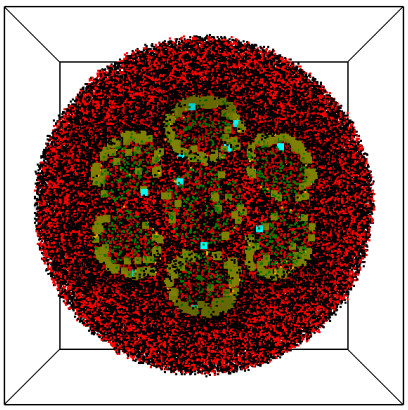

Figure 11: Simulation environment for localized activation. Each small circular region is the size of 1% of the cell surface. pMAP3K is only present in the 7 circular regions.

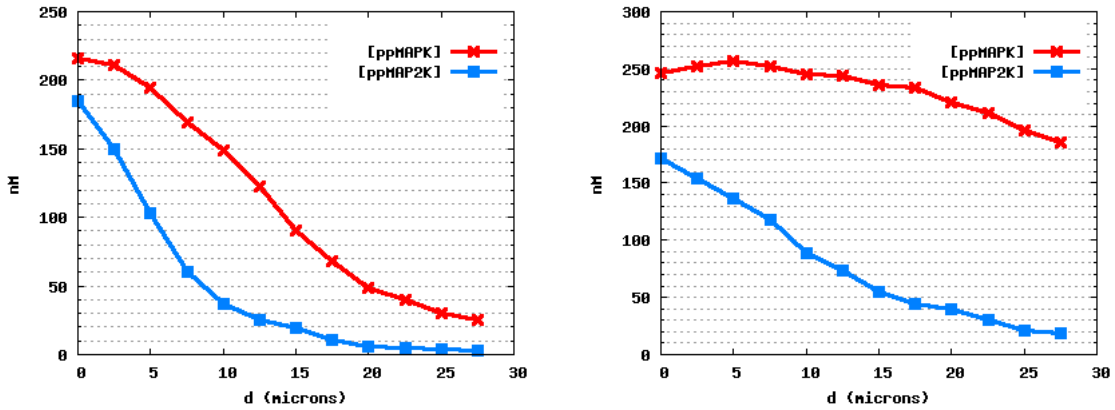

(a) (b)

Figure 12: Steady states for different cases of localized activation of MAP2K on cell surface, [MAP2K P'ase]=10nM. (a): Activation region size of 1% of cell surface. [ppMAP2K] fell below the bistable region at 17μm, resulting in a failed signal propagation. (b): Activation region size of 7% of cell surface. [ppMAP2K] is within or above the bistable region throughout the cell and there is a high concentration of ppMAPK at the nucleus.

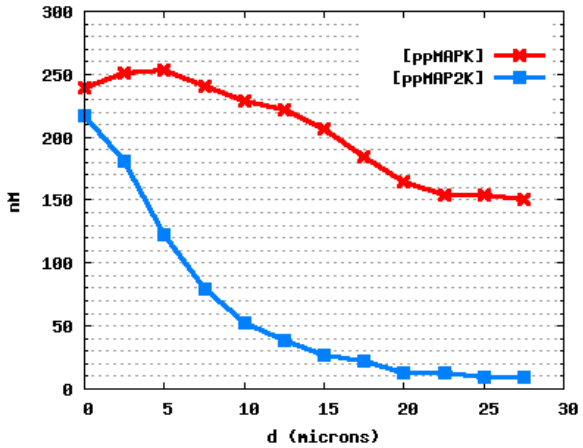

Figure 13: Steady state when pMAP3K is restricted to seven distributed activation regions, each the size of 1% of cell surface, [MAP2K P'ase]=10nM. The signal is weakened at the nucleus but still significant. [ppMAP2K] is within or above the bistable region for 60% of the distance between the surface and the nucleus.

2.8 Alternative Mechanisms

Up to this point it has been seen through stochastic simulations that bistability in the last tier of the MAPK cascade is able to facilitate wave propagation only under certain conditions. For example, bistability alone is unable to accomplish 1-dimensional wave propagation. Markevich et al.[7] proposed two additional mechanisms that can be added to the MAPK cascade that offer solutions to these short comings. Both mechanisms include some form of direct positive feedback, which the cascade model has, so far, lacked.

The first mechanism is inhibition of MAP2K P'ase by ppMAPK, an updated cascade diagram including this mechanism is shown in Figure 14. I implemented this mechanism into the stochastic model by allowing for the formation of a complex between ppMAPK and MAP2K phosphatase. This complex simply forms and breaks apart according to two rate constants. Neither ppMAPK nor MAP2K phosphatase are altered while complexed with each other. The result of such a mechanism is the reduced rate of deactivation of pMAP2K and ppMAP2K because MAP2K P'ase is unable to engage in any other reaction while complexed with ppMAPK.

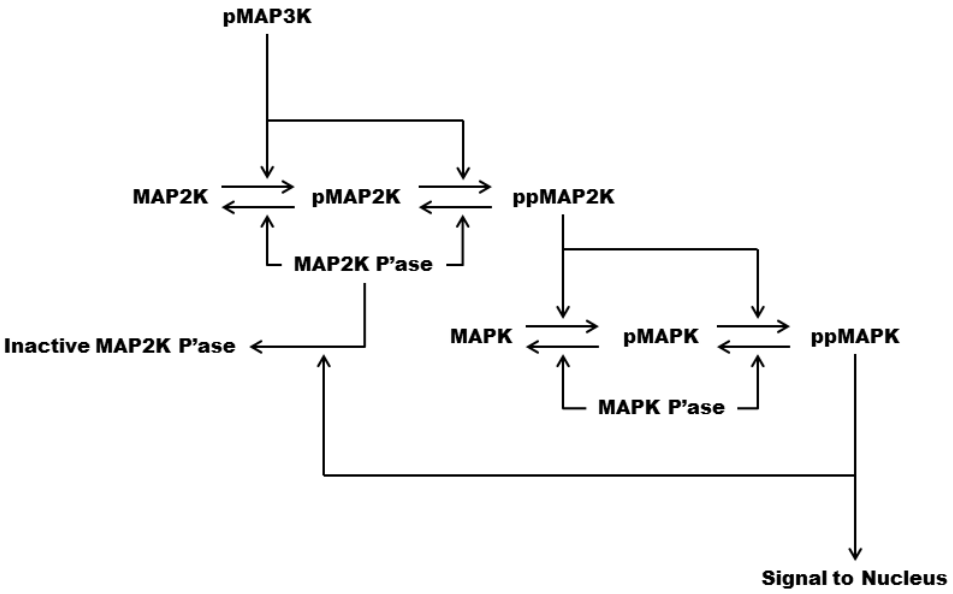

Figure 14: MAPK Cascade with MAP2K P'ase Inhibition

To determine the consequences of the addition of this mechanism, I first confirmed that the inclusion of this feedback indeed transduced the signal under conditions where signal transduction was successful due to bistability alone. Then, I employed the mechanism under conditions where bistability alone failed to propagate a signal. This failure occurred in the case of 1-dimension, spherical geometry with a [ppMAP2K] spatial profile that fell below the bistable region near the nucleus, and small localized activation regions (1% of surface area and 7% distributed) in spherical geometry.

Figures 15-17 contain the steady state results of simulations conducted for different scenarios with the added MAP2K phosphatase inhibition mechanism. I found that in 1-dimension (the long box) the addition of this mechanism alone extended the spatial profile of [ppMAP2K] and [ppMAPK] farther into the box; however, the propagation still eventually died as [ppMAP2K] fell to zero at distances farther away from the activation surface. Similarly, for the case of the small localized activation region (1% of surface area) there was a slight increase in [ppMAP2K] near the nucleus, but it still remained below the bistable region, and hence there was still failure to propagate the signal. For both, the case of high MAP2K P'ase concentration in the cytosol, and the case of distributed small activation regions, there was marked improvement in signal propagation.

The addition of this MAP2K P'ase inhibition mechanism alone facilitated signal transduction in scenarios that had failed prior. Success in wave propagation in these cases was met by substantial increases in [ppMAP2K](well above the bistable region) throughout the entire cell.

The second proposed mechanism of positive feedback is the activation of MAP2K and pMAP2K

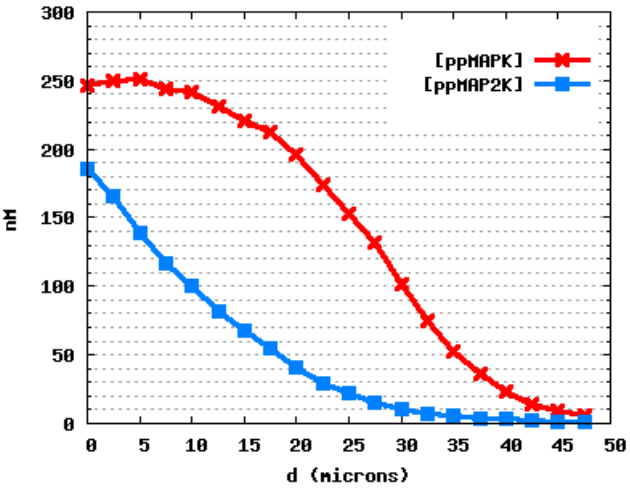

Figure 15: Steady state under the MAP2K P'ase Inhibition mechanism shown in Figure 14. 1-D geometry with [MAP2K P'ase]=24nM. Compared to Figure 5(d) [ppMAP2K] remains within the bistable region at significantly farther distances from the activation surface. Further, [ppMAPK] falls below 200nM at 20μm inward from the surface as compared to 12μm without the additional mechanism.

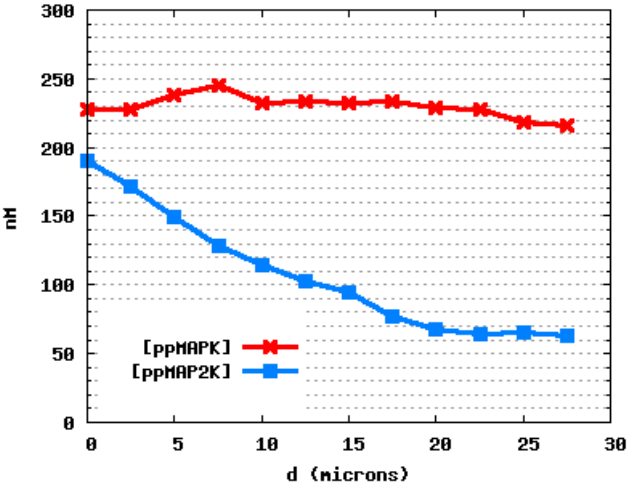

Figure 16: Steady state under the MAP2K P'ase Inhibition mechanism. Spherical geometry with [MAP2K P'ase]=35nM. Compared to Figure 10(b), the addition of this mechanism increased [ppMAP2K] throughout the entire cell to well above the bistable region. Strong signal propagation was successful whereas prior to the addition of the mechanism, propagation failed.

by ppMAPK. This is a significant change in that ppMAP2K can now be created within the cytosol in addition to at the membrane. This mechanism is illustrated in Figure 18.

Once again, after verifying that with the inclusion of this mechanism in the simulations there still occurred signal propagation under conditions where there was previous success, I tested this MAP2K activation feedback under conditions where signal propagation had yet to be achieved. Such conditions are a 1-dimensional wave in a long box, spherical geometry with a high concentration of MAP2K P'ase, and a small localized activation region in spherical geometry.

When testing this mechanism in 1-dimension (the long box), the ppMAPK wave front rapidly propagated through the entire length of the box. The time evolution of [ppMAP2K] and [ppMAPK] throughout the box are shown in Figure 19 and the steady state is provided in Figure 20. The simulations of this mechanism in spherical geometry in both the case with a high MAP2K P'ase concentration, and the case with a small MAP2K activation region on the cell surface, produced similar results in that a non attenuated wave front reached the cell nucleus. While previously, the spreading of ppMAP2K throughout the cytosol occurred through diffusive means only, seen now is the emergence of a wave front

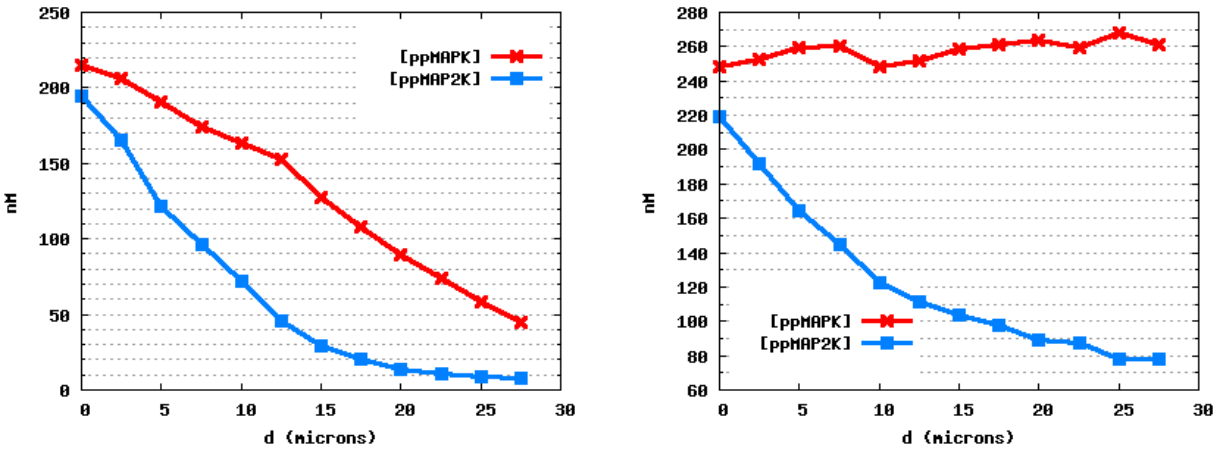

(a) (b)

Figure 17: Steady states under the mechanism of MAP2K P'ase Inhibition where [MAP2K P'ase]=10nM. (a) Spherical geometry with small localized MAP2K activation region (1% of surface area). The addition of this mechanism provided a minor improvement as compared to Figure 12(a), but [ppMAPK] remained low at the cell nucleus. (b) Distributed MAP2K activation regions in spherical geometry (7% of surface area). The addition of this mechanism increased [ppMAP2K] throughout the entire cell to well above the bistable region. Strong signal propagation was successful whereas prior to the addition of the mechanism, propagation was weak, as seen in Figure 13.

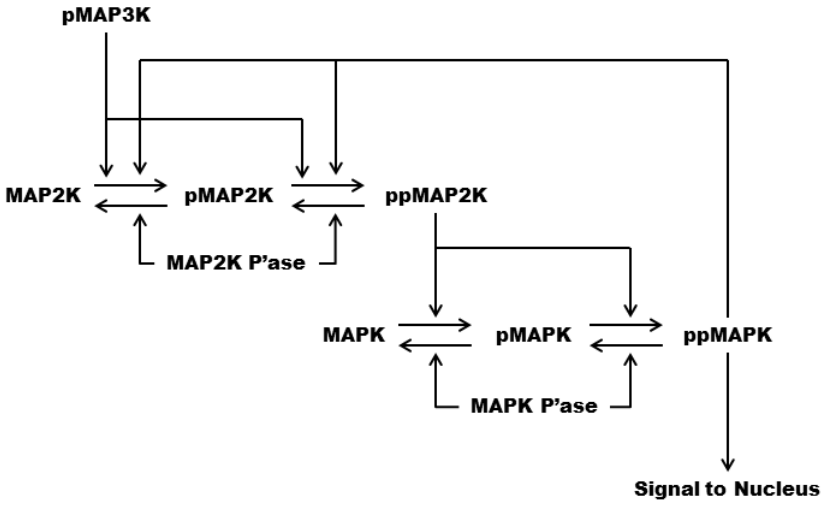

Figure 18: MAPK Cascade with MAP2K Activation Feedback

of [ppMAP2K] that tracks exactly along the wave front of [ppMAPK]. This is a novel characteristic when compared to the previous two mechanisms discussed. The steady state results provided in Figure 21 show that once the waves have propagated through a volume, both [ppMAP2K] and [ppMAPK] are constant throughout that volume, regardless of the initial MAP2K activation location. No longer is there a spatial profile of [ppMAP2K] that falls towards zero with distance from the activation surface.

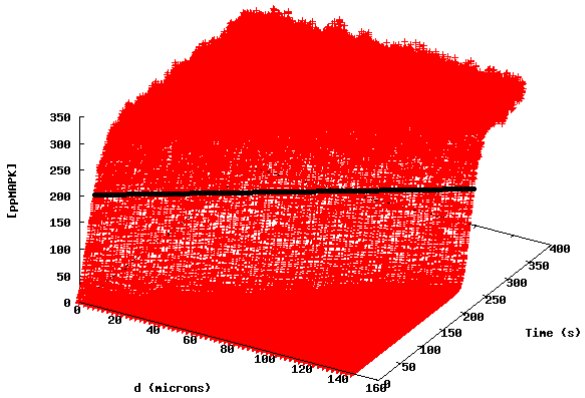

(a)

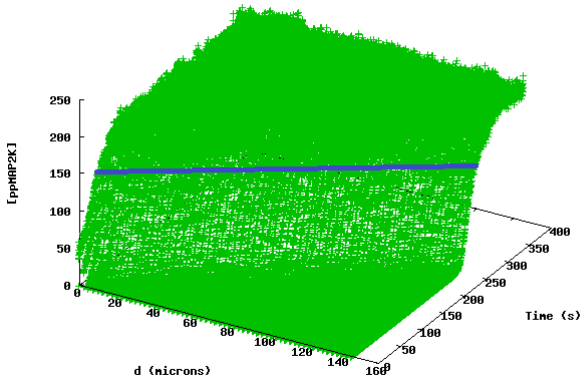

(b)

Figure 19: Time evolution of (a) [ppMAPK] and (b) [ppMAP2K] in 1-dimension, under the MAP2K activation feedback mechanism with [MAP2K P'ase]=24nM. Compared to Figure 5(c). (a) shows a wave that propagated the entire length of the box. (b) shows a new propagating wave front in the concentration of ppMAP2K, a novel characteristic of this mechanism. Contour lines are shown at [ppMAPK]=200nM, and [ppMAP2K]=150nM to display the steady propagation of the waves through the cytosol.

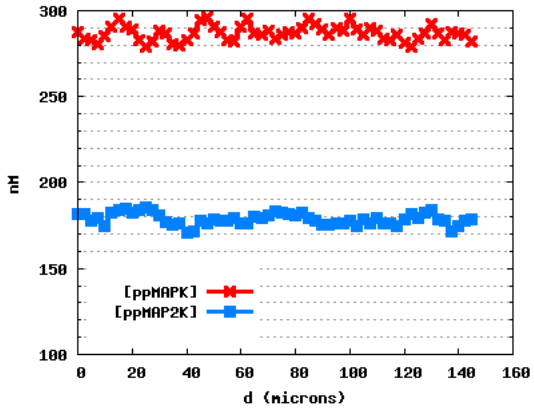

Figure 20: Steady state levels of [ppMAPK] and [ppMAP2K] under the MAP2K activation feedback mechanism in 1-D geometry with [MAP2K P'ase]=24nM.

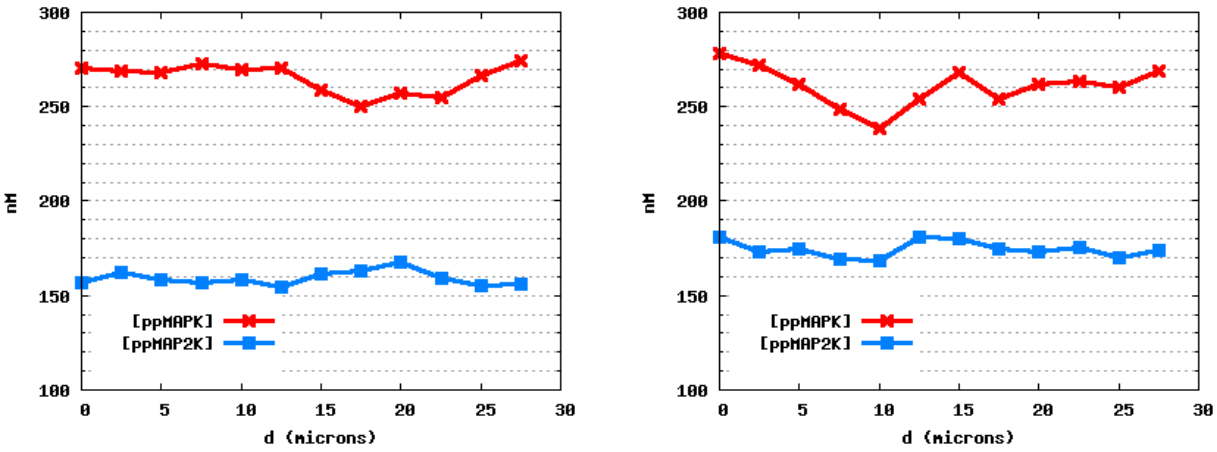

(a) (b)

Figure 21: Steady state levels of [ppMAPK] and [ppMAP2K] under the MAP2K activation feedback mechanism.(a) Spherical geometry with [MAP2K P'ase]=35nM. (b) Spherical geometry with small localized MAP2K activation region (1% of surface area) and [MAP2K P'ase]=10nM.

3 Discussion

In past literature, much emphasis had been placed on the importance of bistability in the MAPK cascade. For this was seen as a necessary condition in order for chemical waves to emerge from such a reaction network. This work focused on whether this property of bistability could be observed in a stochastic simulation, and indeed is has. Further though, was the question of what about bistability provided the possibility of wave propagation. For this signal transduction pathway, the signal was only considered to reach the nucleus if a high concentration of ppMAPK was achieved at the nucleus, meaning a concentration at the nucleus close to the concentration at the cell surface. Therefore, the behavior of this concentration was of great importance for each scenario discussed in the results section. However, what emerged to be equally important was the behavior of [ppMAP2K]. It should be noted that, regardless of the behavior of [ppMAP2K], the bistable characteristic of the final tier of the MAPK cascade was always present; Meaning that, my engineering of the scenarios to achieve different spatial profiles of [ppMAP2K] did not change the bifurcation diagram provided in Figure 3. The statement that bistability allows for wave propagation is not the entire story, for there is clear dependence on the spatial profile of [ppMAP2K] as multiple examples were provided where bistability was present in each, yet signal propagation was unsuccessful.

Seen specifically in the 1-dimensional case is that the propagation of the wave diminishes quickly at distances where [ppMAP2K] falls below the bistable region (<15 nM). Further, for the spherical case [ppMAP2K] had to be in the bistable region sufficiently close to the nucleus (within 10μm) in order for a non-attenuated wave to reach the nucleus. A wave front consisting of a high concentration of ppMAPK is unable to travel far into a region where the steady state concentration of ppMAPK is close to zero.

What bistability does provide however, is a stable steady state consisting of a high concentration of ppMAPK in a solution with a relatively low concentration of its activator, ppMAP2K. The effect of such a property is that a large enough disturbance in an area where [ppMAPK] is low, but also where [ppMAP2K] is within the bistable region can transition [ppMAPK] to the high steady-state. As an example of this transition, Figure 22(a) shows a box separated by a partition. Each side contains the exact same concentration of all molecules, but the left partition was initialized with the high steady state of [ppMAPK] while the right partition was initialized with [ppMAPK] close to zero. [ppMAP2K] throughout the box is constant and was set to 20nM, which is in the bistable region. When kept separate, no change is observed on either side, as expected since both sides are in steady states. However, if the partition is opened, then the entire box transitions to the high steady state of [ppMAPK], shown in Figure 22(b).

In the various simulation performed throughout this study, the disturbance that is able to transition

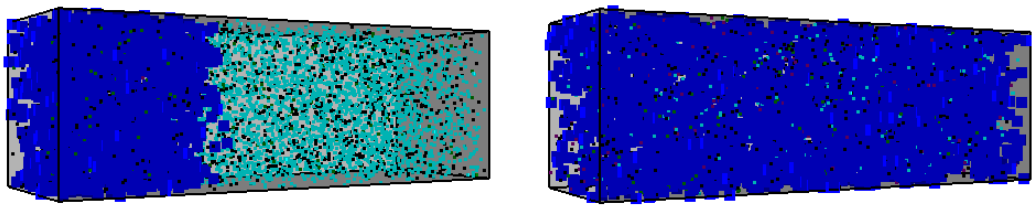

(a) (b)

Figure 22: A disturbance can transition a system to a new steady state, if the system is bistable. Blue squares represent molecules of ppMAPK. The only chemical species present in the box are: ppMAP2K, MAPK, pMAPK, ppMAPK, and MAPK P'ase. [ppMAP2K] is 20nM throughout the box, this places the system in the bistable region, see Figure 3. (a) Both sides are separated by a partition, and are in steady states. The left partition is in the steady state with high [ppMAPK], while the right is in the steady state with low [ppMAPK]. (b) shows the system after the partition is removed. The entire system transitioned to the steady state with high [ppMAPK].

the system to the steady state with high [ppMAPK] is the high concentration of ppMAPK produced at the cell membrane. This high ppMAPK concentration first propagates through areas with a high concentration of ppMAP2K (>30nM) then, into areas where [ppMAP2K] is within the bistable region (15-32nM) and finally halts when [ppMAP2K] fall below the bistable region(<15nM).

The property of bistability extends the concentration range of ppMAP2K that the wave is able to propagate into. This is in contrast to a possibly sigmoidal (ultrasensitive) response, shown in Figure 23(a), where once the wave reached an area with [ppMAP2K] below 40nM it would cease to propagate since the only steady state concentration of ppMAPK in such areas is near zero.

This brings into question a claim made by Markevich et al.[7] that ultrasensitivity was not sufficient for transducing the signal. However, I find in this study that the crucial determinant of propagation lies in the spatial profile of [ppMAP2K]. To reinforce this finding, I constructed a scenario in spherical geometry that had the steady state spatial profile of [ppMAP2K] shown in Figure 7(b). Further, I adjusted the elementary rate constants and the concentration of MAPK phosphatase to transform the bistability of [ppMAPK] to ultrasensitivity, shown in Figure 23(b). Simulation of this scenario showed successful propagation of the signal to the nucleus, as shown in Figure 24.

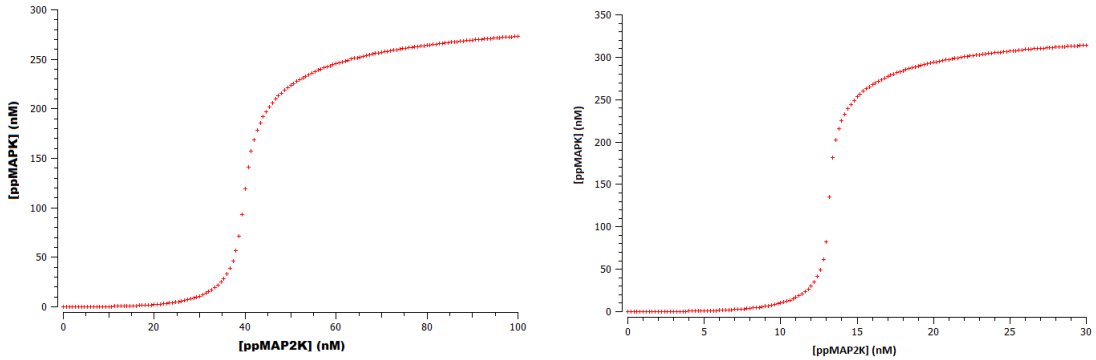

(a) (b)

Figure 23: Wave propagation under ultrasensitivity. (a) Ultrasensitivity after adjusting rate constants. The transition between low and high ppMAPK concentration steady states occurs at [ppMAP2K]=40nM. A wave front of ppMAPK will not propagate into regions of a cell where [ppMAP2K] is below 40nM. (b) Ultrasensitivity after adjusting rate constants and lowering [MAPK P'ase]. By additionally lowering [MAPK P'ase], the steady state transition now occurs at [ppMAP2K]=14nM.

The two alternative mechanisms investigated essentially perform the same task, that is they both alter the spatial profile of [ppMAP2K]. The first mechanism slows the rate of deactivation of pMAP2K and ppMAP2K through the inhibition of MAP2K phosphatase. This simply allows ppMAP2K to

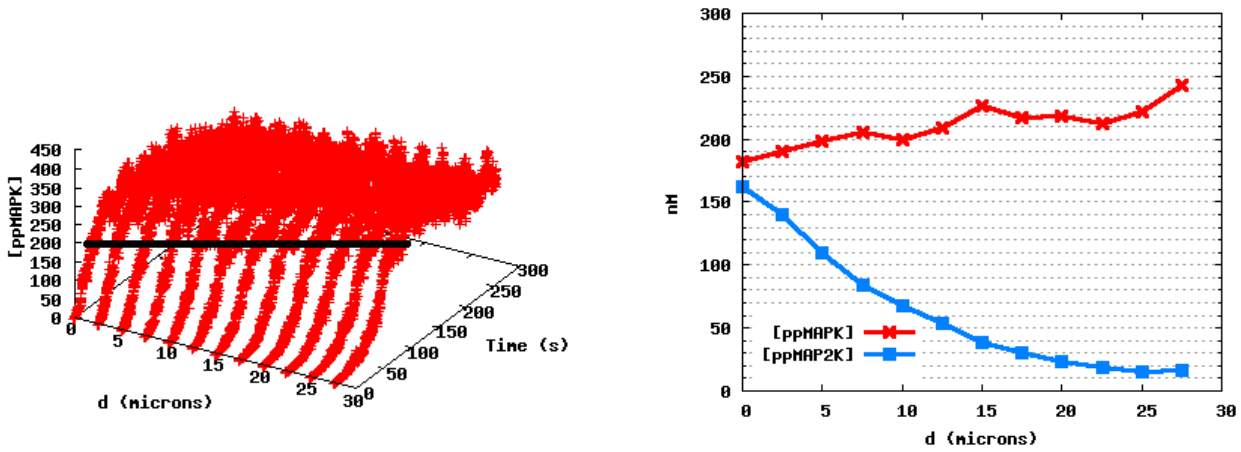

(a) (b)

Figure 24: Wave propagation in spherical geometry, with [MAP2K P'ase]=10nM, under the ultrasensitivity bifurcation shown in Figure 23(b). (a) Time evolution of [ppMAPK]. The contour line at [ppMAPK]=200nM illustrates strong propagation of the wave all the way to the nucleus. (b) Steady states of [ppMAP2K] and [ppMAPK]. [ppMAP2K] remained above 14nM throughout the cell, and therefore the steady state concentration of ppMAPK was high everywhere.

diffuse farther into the cytosol, from the cell membrane. A longer diffusion distance allows for a larger build up in [ppMAP2K] at distances far from the membrane. If the increase is large enough to bring [ppMAP2K] into the bistable region in areas of the cytosol where it previously was not, the signal wave is able to propagate farther than before. The second mechanism is robust in that it creates at the wave front the environment the wave needs to continue propagating. Again, this environment consists of a high concentration of ppMAP2K. This new property allows for sustained signal propagation over much longer distances.

4 Conclusion

Found in this study, through the use of stochastic simulations, was that the major determinant of the success of signal propagation in the MAPK cascade is the steady state spatial profile of the ppMAP2K concentration. For it is the concentration value of this protein that defines spatially where a wave of ppMAPK is able to propagate. In order for a high concentration of ppMAPK to exist in any region of a cell, there must be a sufficient [ppMAP2K] in that same region that supports such a concentration. This is where the role of bistability is found in supporting wave propagation.

First, bistability provides a stable steady state of high [ppMAPK] in a setting of low [ppMAP2K]. Second, under bistability a disturbance is able to transition a low concentration steady state to a high concentration steady state. It it this property that drives the propagation of the wave front through the cytosol.

Additional mechanisms of positive feedback that can be added to the cascade primarily alter the spatial profile of [ppMAP2K]. Specifically [ppMAP2K] is higher in all regions when positive feedback mechanisms are employed than when compared to when only bistability is present. This increase in [ppMAP2K] facilitates wave propagation under conditions where bistability alone was not able to do so. The extreme case is under the MAP2K activation feedback mechanism, where both [ppMAP2K] and [ppMAPK] propagate as wave fronts, allowing for the signal to be carried over much longer distances.

Finally, the dependence, I found, of wave propagation on the spatial profile of [ppMAP2K] suggests that specific bifurcations in a cascade may not be the major limiting or supporting factor in mechanisms such as wave propagation. For above I show that signal transduction is possible under ultrasensitivity as well. This allows for the possibility that other signal transduction pathways may function through wave propagation yet not exhibit bistability. Rather, adjustments in the spatial profile of an upstream activator, ppMAP2K in this case, could reveal novel dynamics in similar reaction networks.

5 Appendix: Simulation and Model Details

Simulations were executed using a program called Smoldyn. This is stochastic simulator with single molecule detail [9], [10]. The total concentrations used for each simulation were the same as used by Markevich et al.[7] which were derived from experiment: $[\text{MAPK}]_{Total}$= 360nM, $[\text{MAP2K}]_{Total}$= 200nM, [MAPK P'ase]= 75nM, and [pMAP3K]= 100nM. In this model, molecules were allowed to diffuse freely through space, each with a diffusion coefficient of $2\mu\text{m}^2/\text{s}$. For bimolecular reactions, in order for two species to react they must be within a specified radius of each other. This radius is set by the reaction rate constant. If two reactants were located within their binding radius then the reaction occurs. After a complex separates into two different chemical species, the two new molecules are immediately placed a distance apart to prevent a second immediate reaction.

The following is the sequence of program operations starting at time = t and ending at time = $t + \delta t$.

1. Observe and manipulate system.
2. Molecules diffuse.
3. Surface and boundary interactions.
4. Reactions in the following order: 0th order, 1st order, and 2nd order.
5. Surface interactions of reaction products.

Tables 2 and 3 provide the reactions and parameters used in the simulations. The chemical kinetics used in the simulations follow the law of mass action. For example, the following equation describes the change in [ppMAPK] in time. This equation is the elementary rate step description (as opposed to Michaelis-Menten kinetics) based off reactions 6 and 7,

$$\frac{d}{dt}[\text{ppMAPK}] = k_6[\text{pMAPK}*\text{ppMAP2K}] + d_7[\text{ppMAPK}*\text{MAPK P'ase}] - a_7[\text{ppMAPK}][\text{MAPK P'ase}].$$

Table 2: MAPK Cascade Reactions

Reaction	Equation
1	$\text{pMAP3K}+\text{MAP2K} \xrightarrow{a_1} \text{pMAP3K}+\text{pMAP2K}$
2	$\text{pMAP3K}+\text{pMAP2K} \xrightarrow{a_2} \text{pMAP3K}+\text{ppMAP2K}$
3	$\text{ppMAP2K}+\text{MAP2K P'ase} \underset{d_3}{\overset{a_3}{\rightleftharpoons}} \text{ppMAP2K}*\text{MAP2K P'ase} \xrightarrow{k_3} \text{pMAP2K}+\text{MAP2K P'ase}$
4	$\text{pMAP2K}+\text{MAP2K P'ase} \underset{d_4}{\overset{a_4}{\rightleftharpoons}} \text{pMAP2K}*\text{MAP2K P'ase} \xrightarrow{k_4} \text{MAP2K}+\text{MAP2K P'ase}$
5	$\text{MAPK}+\text{ppMAP2K} \underset{d_5}{\overset{a_5}{\rightleftharpoons}} \text{MAPK}*\text{ppMAP2K} \xrightarrow{k_5} \text{pMAPK}+\text{ppMAP2K}$
6	$\text{pMAPK}+\text{ppMAP2K} \underset{d_6}{\overset{a_6}{\rightleftharpoons}} \text{pMAPK}*\text{ppMAP2K} \xrightarrow{k_6} \text{ppMAPK}+\text{ppMAP2K}$
7	$\text{ppMAPK}+\text{MAPK P'ase} \underset{d_7}{\overset{a_7}{\rightleftharpoons}} \text{ppMAPK}*\text{MAPK P'ase} \xrightarrow{k_7} \text{pMAPK}+\text{MAPK P'ase}$
8	$\text{pMAPK}+\text{MAPK P'ase} \underset{d_8}{\overset{a_8}{\rightleftharpoons}} \text{pMAPK}*\text{MAPK P'ase} \xrightarrow{k_8} \text{MAPK}+\text{MAPK P'ase}$

Reaction	$a[\text{nmol}^{-1}\text{s}^{-1}]$	$d[\text{s}^{-1}]$	$k[\text{s}^{-1}]$
1	$0.5^*[\text{s}^{-1}]$	-	-
2	$0.5^*[\text{s}^{-1}]$	-	-
3	0.01	0.01	1
4	0.01	0.01	1
5	0.02	0.8	0.1
6	0.032	0.8	15
7	0.045	1	0.092
8	0.01	1	0.5

Table 3: Theoretical MAPK Cascade Reaction Rate Constants

References

[1] Heinrich R, Neel, BG & Rapoport, TA (2002) Mathematical models of protein kinase signal transduction. *Mol. Cell* 9, 957–970.

[2] Huang C, Ferrell JJ (1996) Ultrasensitivity in the mitogen-activated protein kinase cascade. *Proc Natl Acad Sci* USA 93: 10078–10083.

[3] Kholodenko BN (2002) MAP kinase cascade signaling and endocytic trafficking: a marriage of convenience? *Trends Cell Biol.*; 12:173–177.

[4] Kholodenko BN (2003) Four-dimensional organization of protein kinase signaling cascades: the roles of diffusion, endocytosis and molecular motors. *J. Exp. Biol.*; 206:2073–2082.

[5] Ortega F, Garces JL, Mas F, Kholodenko BN, Cascante M (2006) Bistability from double phosphorylation in signal transduction. *FEBS J* 273: 3915–3926.

[6] Markevich NI, Hoek JB, Kholodenko BN (2004) Signaling switches and bistability arising from multisite phosphorylation in protein kinase cascades. *J Cell Biol* 164: 353–359.

[7] Markevich NI, Tsyganov MA, Hoek JB, Kholodenko BN. (2006) Long-range signaling by phosphoprotein waves arising from bistability in protein kinase cascades. *Mol Syst Biol* ;2:61

[8] Zuccaro S, Niedernostheide F-J, Kukuk B, Strych M, Purwins H-G (2000) Solitary current-density patterns in thin ZnS:Mn films. *Physical review. E, Statistical physics, plasmas, fluids, and related interdisciplinary topics*, 62.

[9] Andrews SS,Addy NJ, Brent R, Arkin AP (2010) Detailed simulations of cell biology with Smoldyn 2.1. *PLoS Comp. Biol.* 6:e1000705.

[10] Andrews SS, Bray D (2004) Stochastic simulation of chemical reactions with spatial resolution and single molecule detail. *Phys. Biol.* 1:137-151.